in an additional layer, 130 km thick, when added to the base of the model. The negative anomaly remained unaffected. Standard errors given by the least-squares solution are all ~0.6%. The diagonal elements of the resolution matrix ranged from 0.55 in the top layer to 0.86 in the lowest layer. Average misfit for the final model is 0.297 s.

The Bouguer gravity anomaly calculated for both the polynomial model and the block model shows good agreement with the measured data for the area. Figure 3*d* shows the fit for the gravity values calculated from the polynomial model for which the adjusted density contrast in the low-velocity zone gave a value of $-0.05\ g\ cm^{-3}$, that is, ~1.6% of $3.2\ g\ cm^{-3}$. The ratio of velocity to density contrast, 5.0, is much larger than expected from the Nafe-Drake[24] relationship determined from different types of igneous rock, which gives a value of ~0.8. Such an increase in the sensitivity of velocity to change in density is consistent with the presence of a small fraction of partial melt within the low-velocity zone which, while having little effect on density, will have a disproportionately larger effect on shear modulus and hence P-wave velocity. High attenuation supports this view. P-wave amplitudes measured at Albuquerque, which lies on the rift, are among the most attenuated of those measured at standard stations in the United States[25]. Greater attenuation is seen only at Golden, Colorado, to the north, on the Rocky Mountain front.

The topography also agrees qualitatively with that in isostatic balance with the polynomial model, that is, in thermal isostatic equilibrium. Therefore, the model we assume to explain the teleseismic delays, attenuation[25], gravity, uplift[14,15], regional heat flow[26] and the presence of rifting and volcanism, is based on a hot, low-density asthenospheric body which has replaced the lithosphere by upward movement of the lithosphere-asthenosphere boundary. Such migration of the melting point geotherm might be caused by either lithospheric extension[10] or active convection[27] in the upper mantle and requires further quantitative work to elucidate the mechanism. Nonetheless, the boundary has a configuration expected to exist in a region as a prelude to the opening of oceans and continental drift. Although the polynomial fit of Fig. 3*b* shows some agreement with lithospheric depths determined from Rayleigh waves, other points are still unresolved. Where low P-wave velocities have been associated with low S-wave velocities[9,28,29] in the low-velocity zone, the per cent reduction in P-velocity is about half that in S-velocity. Our model reduction in P-velocity is −8%, implying an unprecedented regional reduction of S-velocity of −14%. Also, the low-velocity zone has been associated with increased density values[7,28], which is opposite to our conclusion. If we compromise between less P-wave velocity perturbation and increased amplitude of the variation of the boundary, the flanks would be placed too deep for them to interface with surface wave models of lithospheric thickness. Therefore, if asthenospheric upwarp is to explain the gravity, topography and teleseismic delays, the properties of the asthenosphere in this region must differ from those encountered elsewhere. However, we might expect this, as it underlies the most negative region of the east-west, continental Bouguer gravity profile (latitude 37°, Fig. 1).

This work was supported by grants from the University of California, Los Angeles, and the Institute of Geophysics and Planetary Physics at Los Alamos National Laboratory.

Received 7 August; accepted 5 September 1984.

1. Morgan, P. & Baker, B. H. *Tectonophysics* **94**, 1-4 (1983).
2. Parker, R. L. & Oldenburg, D. W. *Nature* **242**, 137-139 (1973).
3. Oldenburg, D. W. *Geophys. J.R. astr. Soc.* **43**, 425-451 (1975).
4. Schubert, G., Froidevaux, C. & Yuen, D. A. *J. geophys. Res.* **81**, 3525-3540 (1976).
5. Davis, P. M. *Nature* **308**, 53-55 (1984).
6. Knopoff, L. *Tectonophysics* **13**, 497-519 (1972).
7. Biswas, N. N. & Knopoff, L. *Geophys. J.R. astr. Soc.* **36**, 515-540 (1974).
8. Priestley, K. & Brune, J. *J. geophys. Res.* **83**, 2265-2272 (1978).
9. Priestley, K., Orcutt, J. A. & Brune, J. N. *J. geophys. Res.* **85**, 7166-7174 (1980).
10. McKenzie, D. *Earth planet. Sci. Lett.* **40**, 25-32 (1978).
11. Sleep, N. H. *Geophys. J.R. astr. Soc.* **24**, 325-350 (1971).
12. Steckler, M. S. & Watts, A. B. in *Dynamics of Passive Margins, Geodynamics Ser.* Vol. 6, 184-196 (Am. Geophys. Un., Washington, D.C., 1982).
13. Ramberg, I. B., Cook, F. A. & Smithson, S. B. *Bull. geol. Soc. Am.* **89**, 107-123 (1978).
14. Cordell, L. *Bull. geol. Soc. Am.* **89**, 1073-1090 (1978).
15. Ander, M. E. thesis, Univ. New Mexico (1980).
16. Iyer, H. M. *Nature* **253**, 425-427 (1975).
17. Aki, K. *Rev. Geophys. Space Phys.* **20**, 161-170 (1982).
18. Iyer, H. M. *Phil. Trans. R. Soc.* **A310**, 473-510 (1984).
19. Evans, J. R. *J. geophys. Res.* **87**, 2654-2670 (1982).
20. Herrin, E. *Bull. seism. Soc. Am.* **58**, 1196-1219 (1968).
21. Davis, P. M., Parker, E. C., Evans, J. R., Iyer, H. M. & Olsen, K. H. in *New Mexico Geological Society Guidebook* (New Mexico Geol. Soc., Socorro, New Mexico, 1984).
22. Aki, K., Christofferson, A. & Husebye, E. S. *Bull. seism. Soc. Am.* **66**, 501-524 (1976).
23. Ellsworth, W. A. thesis, Massachusetts Inst. Technol. (1977).
24. Ludwig, W. J., Nafe, J. E. & Drake, C. L. *The Sea* Vol. 4, 53-84 (Wiley, New York, 1970).
25. Butler, R. *Rev. Geophys. Space Phys.* **22**, 1-36 (1984).
26. Rieter, M., Mansure, A. J. & Shearer, C. in *Rio Grande Rift: Tectonics and Magmatism* (ed. Rieker, R. E.) 253-268 (Am. Geophys. Un., Washington, D.C., 1979).
27. Sengor, A. M. C. & Burke, K. *Geophys. Res. Lett.* **5**, 419-421 (1978).
28. Dziewonski, A. M., Hales, A. L. & Lapwood, E. R. *Phys. Earth planet. Inter.* **10**, 12-48 (1975).
29. Burdick, L. J. & Helmberger, D. V. *J. geophys. Res.* **83**, 1699-1712 (1978).

Enhanced preservation of marine-derived organic matter in Cenomanian black shales from the southern Angola Basin

P. A. Meyers*, M. J. Leenheer†, O. E. Kawka*‡ & T. W. Trull*‡

* Department of Atmospheric and Oceanic Science, University of Michigan, Ann Arbor, Michigan 48109, USA
† Cities Service Technology Center, PO Box 3908, Tulsa Oklahoma 74102, USA

Black shales possessing high concentrations of organic carbon[1] were deposited in many parts of the proto South Atlantic Ocean during the Cretaceous period[2]. The way such sediments accumulated is not fully understood, but is likely to have occurred through a combination of low oxygen availability and abundant supply of organic matter. Thin, centimetre-thick layers of black shales are commonly interbedded with thicker layers of organic carbon-deficient, green claystones, as found in strata of Aptian to Coniacian age, at Deep Sea Drilling Project (DSDP) Site 530, in the southern Angola Basin[3] and elsewhere. These differences in carbon content and colour reflect the conditions of deposition, and possibly variations in the supply of organic matter[4,5]. We have compared, using organic geochemical methods the compositions of organic matter in three pairs of closely-bedded black and green Cenomanian claystones obtained from Site 530. Kerogen analyses and distributions of biological markers show that the organic matter of the black shales is more marine and better preserved than that of the green claystones.

The results of the analyses are presented in Table 1. X-ray diffraction studies do not show any significant differences between the mineralogical contents of the black and green claystones. Furthermore, the pyrite content of adjacent intervals is similar: its relative abundance seems to depend more on the depositional setting than on the amount of organic matter in the sediments.

Values of total organic carbon, however are significantly higher for the black shales than for their green claystone pairs. Modern deep-sea sediments generally contain ~0.2% organic carbon[6]. Values as high as in these black shales are found in only a few areas of present-day oceans[7], which are under anoxic or poorly oxygenated bottom-waters. A rare combination of abundant supply and exceptionally good preservation of organic matter is needed for such organic carbon-rich sediments to accumulate.

Visual kerogen analysis of the green and black claystones shows that both contain two populations of vitrinite and amorphous kerogen. Whereas the indigenous vitrinite content indicates that the samples are thermally immature, Fig. 1 shows that the green claystones differ from the black shales in containing a larger amount of recycled vitrinite having a higher thermal

‡ Present addresses: School of Oceanography, Oregon State University Corvallis, Oregon 93701, USA (O.E.K.); Woods Hole Oceanographic Institution, Woods Hole, Massachusetts 02543, USA (T.W.T.).

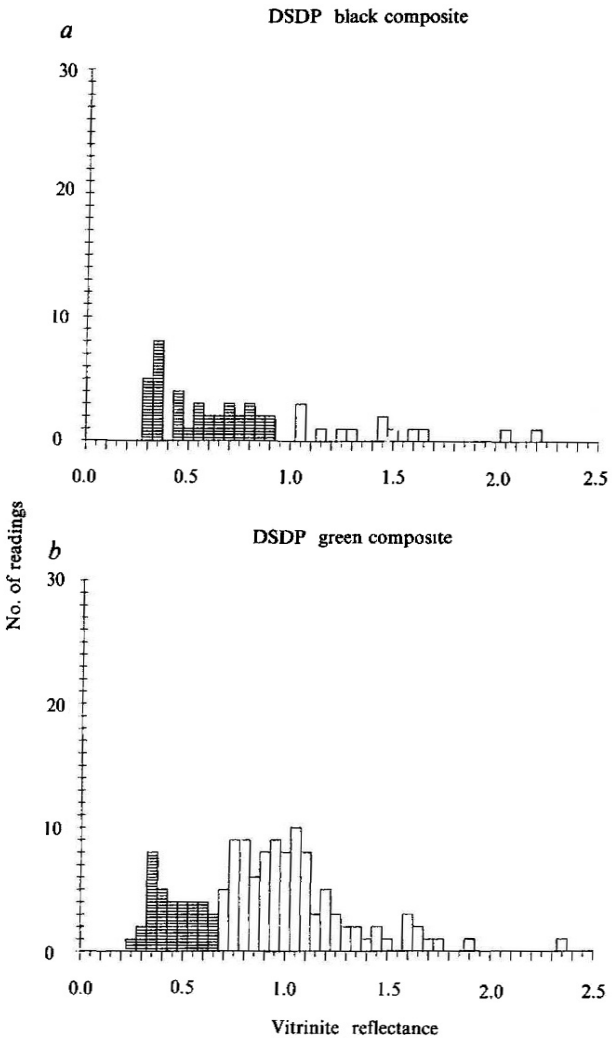

Fig. 1 Vitrinite reflectance histograms of composite samples of Cenomanian black shale (*a*, mean = 0.545, median = 0.535, s.d. = 0.195, count = 37) and green claystone (*b*, mean = 0.457, median = 0.450, s.d. = 0.113, count = 35) from DSDP Site 530 in the Angola Basin. Hatched area respresents indigenous population.

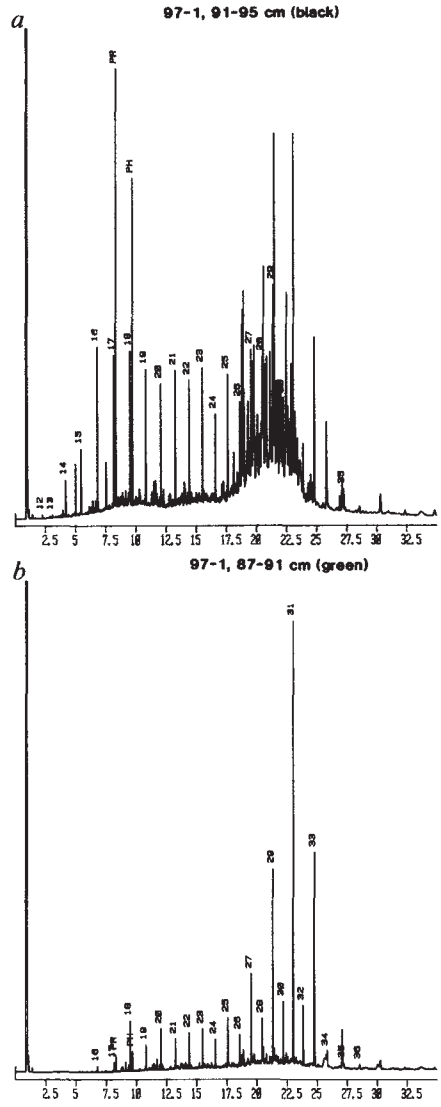

Fig. 2 Gas chromatograms showing extractable aliphatic hydrocarbon distributions of adjacent samples of black (*a*) and green (*b*) claystones from Hole 530A. Pristane and phytane are identified as PR and PH, respectively, and *n*-alkanes by their carbon numbers.

maturity. Similarly, populations of spores present in the green claystones range from transparent to dark orange, indicating a wide range of thermal maturities, whereas the black claystones contain primarily light-coloured, thermally immature spores. Also the amorphous kerogen of the green claystone is ~85% fluorescent compared with 100% in the black shales. Because thermally immature amorphous kerogen is highly fluorescent, the lower percentages in the green claystones suggest they contain a significant amount of nonfluorescing detrital material. The presence of two populations of both vitrinite and amorphous kerogen, indicated as in Fig. 1 by the vitrinite reflectance histograms, and by visual inspection, implies there are differences in the organic matter intake and preservation of the two claystones.

The mean value of organic matter C/N atomic ratios is much greater for the black shales (38.1) than for the green claystones (5.7) and is typical of C/N ratios of cellulosic land-plant organic matter[8]. The ^{13}C content of organic matter in black shales from Site 530 is generally less than in green claystones. This difference in isotopic compositions could mean there is a larger component of land-derived organic material in the black than in the green strata. Characterization of organic matter by kerogen analysis, however, shows that the black shales of the Angola Basin contain more amorphous kerogen, indicative of their aquatic origin, than do the green claystones[10–12].

The contradictions in the identification of the source of organic matter, apparent between the C/N ratios and carbon isotope content and the kerogen analyses may arise from selective preservation of organic matter components. Although preservation is generally high in the black shales, nitrogeneous materials appear to have been selectively lost, thus enhancing C/N ratios. Similarly, classes of organic compounds relatively rich in ^{13}C, such as amino acids and carbohydrates, may have been selectively degraded, as reported in sediments from Mangrove Lake[3], resulting in reduced ^{13}C in the residual organic matter of the black shales. Poorer preservation in the green claystones has led to losses of all but the most resistant forms of organic matter.

Geolipid data agree with this picture of selective preservation. Concentrations of total hydrocarbons, fatty acids, and fatty alcohols are significantly greater in the black shales than in the adjacent claystone (Table 1), yet these geolipids often constitute a smaller fraction of the total organic matter in black shales than in green claystones[14], which is consistent with greater preservation of the more degradable, non-lipid organic matter components in the black shales.

The hydrocarbons in the samples are a combination of compounds either introduced as such to the sediments or generated during diagenesis. The large amounts of aliphatic and aromatic hydrocarbons, in contrast to the smaller amounts of alkanols

Table 1 Comparisons of adjacent Cenomanian black shales with green claystones from DSDP Hole 530A in the Angola Basin

Characteristic of sample	Sample pairs 530A-95-5 0-21 cm	530A-95-5 38-50 cm	530A-97-1 87-91 cm	530A-97-1 91-95 cm	530-97-1 99-105 cm	530-97-1 105-110 cm
Colour	Green	Black	Green	Black	Black	Green
% Calcium carbonate	2	9	5	7	6	6
% Pyrite	4	17	6	6	14	16
% $C_{organic}$	0.2	12.9	0.6	4.9	10.0	0.8
Atomic C/N	4.5	36.0	6.8	38.1	40.3	5.7
% Amorphous kerogen	60	98	60	98	95	90
% Vitrinite-intertinite	40	2	40	2	5	10
Aliphatic hydrocarbons (p.p.m.)	4	274	20	64	135	18
Aromatic hydrocarbons (p.p.m.)	6	695	20	202	284	126
Alkanoic acids (p.p.m.)	3	7	2	6	11	3
Alkanols (p.p.m.)	0.4	5	2	5	9	3

Samples for geochemical comparison, taken from ~1,020 m sub-bottom depth, were selected onboard ship and immediately frozen to protect their organic matter. Analysis of organic carbon and of solvent-extractable geolipids were done as described elsewhere[14]. Kerogen was isolated by demineralization and flotation, and analysed microscopically in both transmitted and reflected light. Bulk minerology was determined by X-ray diffraction.

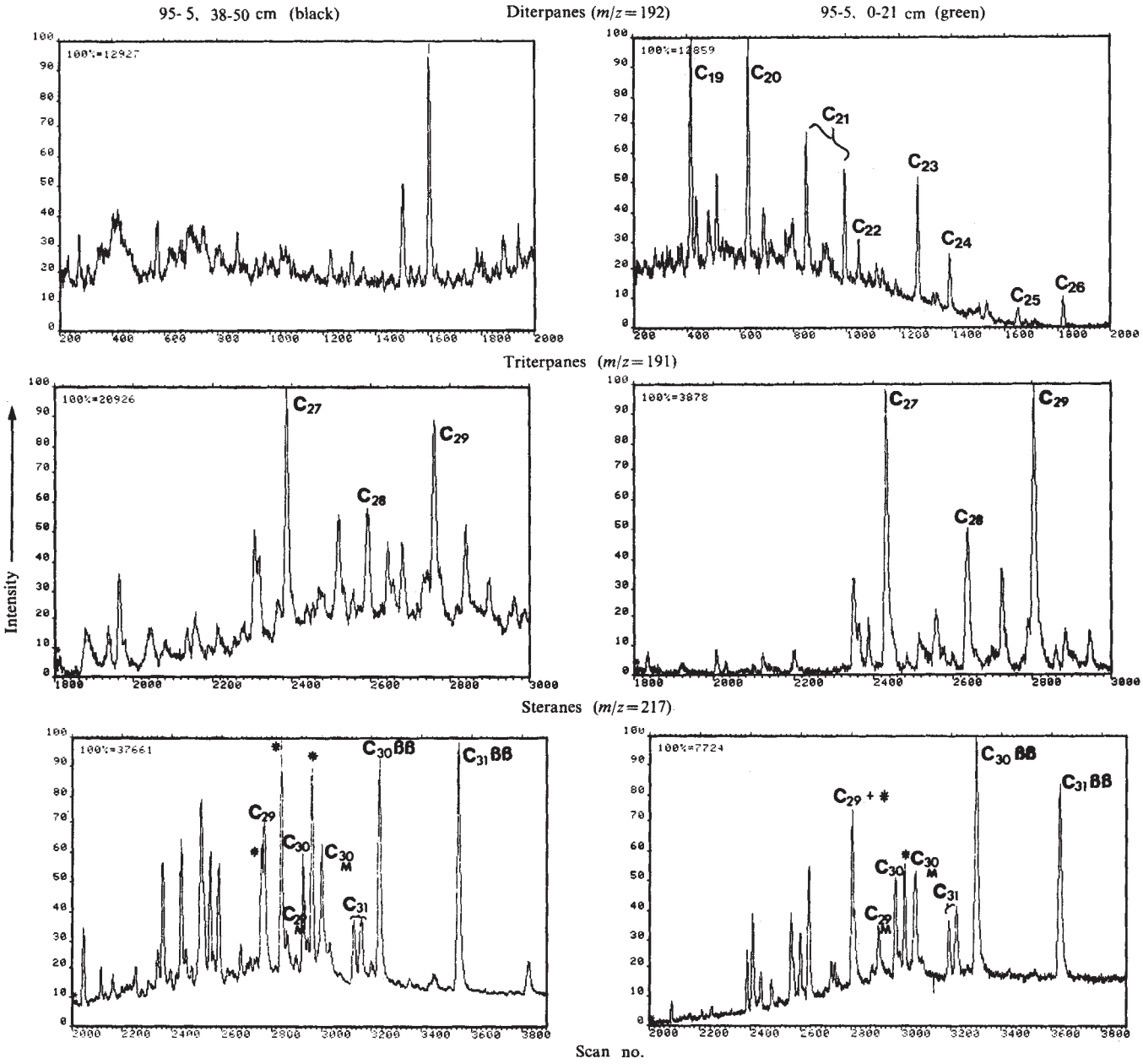

Fig. 3 GC-MS mass fragmentograms of steranes, triterpanes, and diterpanes extracted from black and green claystones from DSDP Hole 530A. The labelled steranes possess unaltered biological 5-α(H), 20-*R* configurations. The C_{29} to C_{31} triterpanes have 17-α(H), 21-β(H) configurations unless labelled as BB. Hopenes are indicated by *, and moretanes (17-β(H), 21-α(H) configurations) by M.

and alkanoic acids in all samples, suggest that a significant amount of these components were generated after deposition and, hence, may reflect diagenetic processes rather than selective preservation as suggested for the more labile compounds. Whereas both types of sample have relatively large amounts of long chain ($>C_{25}$) *n*-alkanes with a pronounced odd-carbon preference, suggesting terrigenous input, Fig. 2 shows that the black claystones also contain significant amounts of shorter chain *n*-alkanes and branched and cyclic hydrocarbons, which are not present in the green claystones[14,15]. These aliphatic hydrocarbons and the larger quantities of C_{27} relative to C_{29} sterane, which are more evident in the black than in the green claystones (Fig. 3), suggest somewhat more aquatic input to the black claystone. In addition, the presence of diterpanes, predominantly C_{19} and C_{20}, in the green claystone, which are absent from the black claystone (Fig. 3) suggests the input of mostly terrigenous, microbially-altered material to the green claystone[16,17]. The unidentified peaks in the m/z 191 trace of the black claystone probably represent tetracyclic terpanes of unknown origin. Hence, the hydrocarbon analysis agrees with the character of the organic matter intake suggested by the visual kerogen analysis.

The triterpane distributions are quite similar (Fig. 3): both types of sample exhibit abundant 17-β(H), 21-β(H)-hopanes which indicate a low degree of thermal maturity[18]. Both the triterpanes present and the occurrence of predominantly biological configurations (that is, 14-α(H), 17-α(H), 20-*R*)[16] of the steranes support the low maturity indicated by vitrinite reflectance and spore colourations, and confirms that the recycled populations do not significantly contribute to the lipid content of these samples.

Comparison of distributions of *n*-alkanoic acids and *n*-alkanols reveals that the black shales contain relatively greater proportions of terrigenous than of marine components of these geolipid classes[14]. Because acids and alcohols are more subject to degradation than hydrocarbons, the difference in source character for these geolipid classes again suggests that selective preservation has occurred in the black shales.

The comparisons of organic matter contents confirm that black shales at DSDP Site 530 in the Angola Basin record periods of enhanced preservation of marine, as well as terrigenous, organic material which is superimposed on a low background of residual land-derived material[15]. Adjacent green claystones exhibit evidence of burrowing benthic animals and show that bottom waters must have been oxic in Cretaceous times[3,19]. Because these Cenomanian sediments contain abundant turbidite sequences, the black shales probably represent episodes of downslope redeposition of sediments originally laid down in a midwater anoxic layer which impinged on the African continental slope[19,20]. Such sediments, rich in organic matter from high marine productivity, must have been rapidly redeposited in the Angola Basin in order to preserve organic substances in an oxic environment. An important implication of this scenario is that deep-ocean black shales can result from local or regional events of short duration which do not involve global oceanic anoxia.

Received 27 February; accepted 13 September 1984.

1. Foresman, J. B. *Init. Rep. DSDP* **40**, 557-567 (1978).
2. Bolli, H. M. *et al. Init. Rep. DSDP* **40**, 357-455 (1978).
3. Hay, W. W. *et al. Bull. geol. Soc. Am.* **93**, 1038-1050 (1982).
4. Summerhayes, C. P. & Masran, T. C. *Init. Rep. DSDP* **76**, 469-480 (1983).
5. Dean, W. E. & Gardner, J. V. in *Nature and Origin and Cretaceous Carbon-rich Facies* (eds Schlanger, S.O. & Citas, M. B.) 55-78 (Academic, London, 1982).
6. Degens, E. T. & Mopper, K. in *Chemical Oceanography* 2nd edn (eds Riley, J. P. & Chester, R.) **5**, 59-113 (Academic, London, 1976).
7. Demaison, G. J. & Moore, G. T. *Org. Geochem.* **2**, 9-31 (1980).
8. Muller, P. J. *Geochim. cosmochim. Acta* **41**, 756-776 (1977).
9. Nohara, M., Ishizuka, T. & Gieskes, J. M. *Init. DSDP* **75**, 1951-1054 (1984).
10. Deroo, G., Herbin, J. P. & Huc, A. Y. *Init. Rep. DSDP* **75**, 983-999 (1984).
11. Rullkotter, J., Mukhopadhyay, P. K. & Welte, D. H. *Init. Rep. DSDP* **75**, 1069-1087 (1984).
12. Katz, B. L. *Init. Rep. DSDP* **75**, 1031-1034 (1984).
13. Hatcher, P. G., Spiker, E. C., Szeverenyi, N. M. & Maciel, G. E. *Nature* **305**, 498-501 (1983).
14. Meyers, P. A., Trull, T. W. & Kawka, O. E. *Init. Rep. DSDP* **75**, 1009-1018 (1984).
15. Brassell, S. C. *Nature* **305**, 1019-1030 (1983).
16. Simoneit, B. R. T. *Geochim. cosmochim. Acta* **41**, 463-476 (1977).
17. Aquino Neto, F. R., Trendel, J. M., Restle, A., Connan, J. & Albrecht, P. A., in *Advances in Organic Geochemistry 1981* (ed. Bjorøy, M. 659-667 (Wiley, Chichester, 1983).
18. Mackenzie, A. S. *et al. Geochim. cosmochim. Acta* **44**, 1709-1721 (1980).
19. Dean, W. E., Arthur, M. A. & Stow, D. A. V. *Init. Rep. DSDP* **75**, 819-844 (1984).
20. Thiede, J. & van Andel, T. H. *Earth planet. Sci. Lett.* **33**, 301-309 (1977).

A model of estuarine circulation in the Pliocene Mediterranean based on new ostracod evidence

Dick van Harten

Geological Institute, University of Amsterdam, Nieuwe Prinsengracht 130, 1018 VZ Amsterdam, The Netherlands

The recent discovery of the psychrospheric ostracod *Agrenocythere pliocenica* (Seguenza) in Zanclean marls of eastern Crete[1] expands the reach of early Pliocene deep-oceanic circulation far into the eastern Mediterranean. Current models of Pliocene water-mass circulation, though allowing for the Atlantic psychrosphere to flow freely into the western basin, consider the eastern basin as being largely stagnant[2,3]. I propose here a new model of estuarine circulation affecting both west and east Mediterranean. This circulation was associated with increased atmospheric humidity and driven by upwelling. The model is compatible with organic-rich sedimentation in parts of the eastern Mediterranean and does not imply an excessively deep or wide connection with the Atlantic.

The term 'psychrosphere'[4] denotes, in an ecological sense, the cold (temperatures <8–10 °C), dense bottom-waters of the world ocean that are directly derived from the polar regions. The benthic ostracods inhabiting this environment include a group of highly characteristic genera, among them *Agrenocythere*, whose occurrence is virtually restricted to these waters. The depth at which these ostracods occur is generally >500 m (ref. 2). In lower latitudes, they live at greater depth than in higher latitudes and upwelling regions[5]. *Agrenocythere* is typical of the upper psychrosphere: recent species are most likely to be found at depths of 1,000–1,500 m; the known depth range of the genus is 400–3,850 m (ref. 6).

In the modern Mediterranean, the temperature of deep bottom-water is ~13 °C[7]. Hence, recent faunas of this sea do not exhibit any typically psychrospheric ostracods. However, several such forms are recorded from Pliocene and earlier sediments in the Mediterranean region[5]. Figure 1 shows *A. pliocenica* found in Crete[1] which supports an earlier, doubtful identification of a single specimen in the Zanclean of DSDP Site 378 in the south Aegean[8]. All other spots where this species has been found lie much more to the west[8-10]; Sicily and southern peninsular Italy are the easternmost localities known so far. This new find eliminates any doubt that Pliocene psychrospheric circulation did press far into the east Mediterranean.

A. pliocenica first appeared in the Mediterranean in the *Globorotalia margaritae* zone (see Fig. 2 for the epochs, stages and biozones mentioned in this paper). In Italy, this species ranges up to the early Pleistocene[9]. In Crete, we have found it

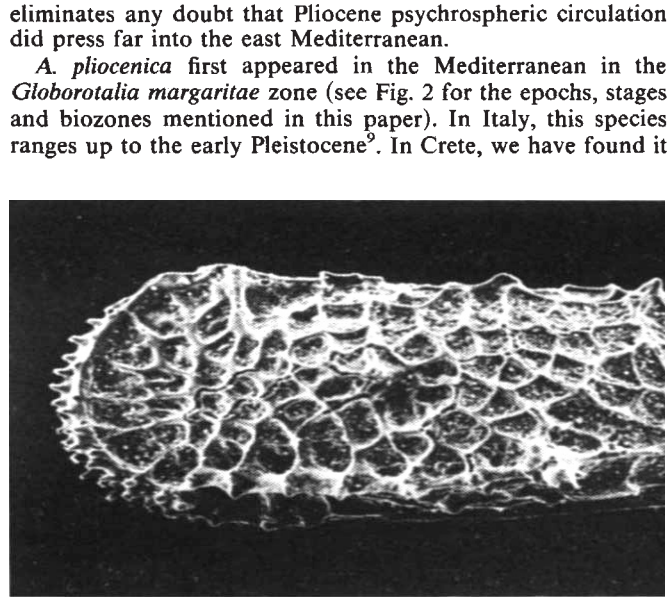

Fig. 1 *A. pliocenica* (Seguenza) from Zanclean marl (*G. margaritae* zone), Xerokambos, southeastern Crete, Greece. Left valve of a male. Length of specimen 1.4 mm.